FAULT IDENTIFICATION IN ROTOR/MAGNETIC BEARING SYSTEMS USING DISCRETE TIME WAVELET COEFFICIENTS

Iain S. Cade, Patrick S. Keogh and M.Necip. Sahinkaya
Department of Mechanical Engineering
University of Bath, BA2 7AY, UK
I.S.Cade@bath.ac.uk

ABSTRACT

A method of online fault identification in rotor/magnetic bearing systems is presented using wavelet analysis. A filter bank approach is taken to identify the discrete time wavelet coefficients of the rotor displacement signals. From artifacts present in the discrete time wavelet series associated with specific faults, it is shown that it is possible to identify both the onset time and the fault type. This method is demonstrated for simulations of a flexible rotor/active magnetic bearing assembly during auxiliary bearing contact and direct synchronous forcing for a range of running speeds covering flexural critical speeds.

INTRODUCTION

Rotor/magnetic bearing systems exist in a wide range of applications and may experience input disturbances giving rise to transient rotor vibration. The origin of a disturbance may arise during normal operating conditions or as a direct result of a fault. Examples of disturbance include unbalance changes, flow induced forces, base acceleration and sensor malfunction. It is important to be able to identify the onset, duration and type of disturbance in order to maintain safe operation of a rotor/magnetic bearing system. This is required to ensure that appropriate control forces are applied to the rotor to restore the system to an operating condition within acceptable bounds.

Sufficient control forces in a fault condition can be evaluated using either a control strategy ensuring stability under open loop failure or by changing the control strategy itself. Cole *et al* [1] present a method of fault tolerant control through the use of a neural network to identify faults and reconfigure an H_∞ control strategy to deal with the fault. Seo and Kim [2] focus on the design of an H_∞ control strategy robust to linear time-varying parameter uncertainty and actuator failure. The work of Gündes [3] presents a design method ensuring system stability during failure of actuators and sensors.

A wide variety of model-based approaches have been taken to identify faults. Sauter and Hamelin [4] consider a method of fault identification from residuals. Increased residual robustness is achieved with frequency-domain fault-detection filtering, where the effect of the filter is to optimize the ratio of magnitudes between fault and disturbance. Maki and Loparo [5] offer a neural network approach to fault detection, which has advantages since little understanding of the system is required. It is also applicable to systems with nonlinearities. Bachschmid *et al* [6] present a method of multiple fault identification by means of model-based identification in the frequency domain.

Analysis of rub-impact faults using the continuous wavelet transform has been studied by Peng *et al* [7]. This method identifies key structure associated with a rub-impact event. Lin and Qu [8] also consider a method of fault diagnosis using feature extraction with the Morlet wavelet in order to remove noise from the signal. This approach utilizes the ability of wavelets to remove noise from a signal rather than provide fault identification in the wavelet domain. A wavelet approach to vibration analysis is presented by Newland [9] allowing for a time-frequency map presentation of a signal with a changing spectral density from which an understanding of the signal vibration can be made.

This paper focuses on the use of wavelet analysis to detect faults in rotor/magnetic bearing systems. A method of feature extraction from the discrete time wavelet series is introduced in order to identify fault onset and type.

SYSTEM MODEL

A flexible rotor model may be derived from finite element analysis to give an equation of motion of the form:

$$\mathbf{M}\ddot{\mathbf{q}} + (\Omega\mathbf{G} + \mathbf{C})\dot{\mathbf{q}} + \mathbf{K}\mathbf{q} = \mathbf{D_f}\mathbf{f} + \mathbf{D_u}\mathbf{u} \qquad (1)$$

where $\mathbf{q}$ is the coordinate vector of the rotor in the reference frame relative to the base and containing displacements in the x and y directions and the angular displacements about them. The x and y axis are arranged orthogonally at an angle of $\pm 45^o$ to the horizontal and vertical

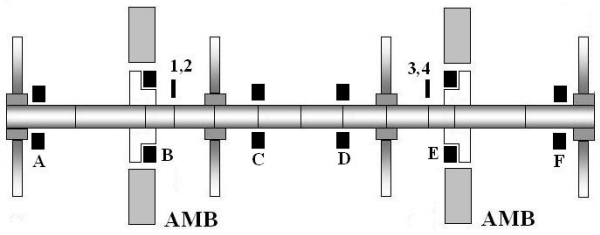

FIGURE 1: Rotor/active magnetic bearing (AMB) configuration showing auxiliary bushes (A,C,D,F) and auxiliary bearings (B,E). Displacement sensors measuring rotor displacement relative to base motion are shown at 1,2,3,4. Finite beam discretization is also shown.

respectively. **f** represents the force vector acting on the rotor and **u** is the control force vector applied to the rotor. **M**,**C**,**K** and **G** represent the mass, damping, stiffness and gyroscopic matrices respectively. $\mathbf{D_f}$ and $\mathbf{D_u}$ are force distribution matrices, which increase the dimensions of **f** and **u** to those of **q**.

A rotor/magnetic bearing system was configured from a flexible rotor with four disks, supported by two active magnetic bearings. A finite element model was constructed from 12 elements with a total of 52 degrees of freedom, finite element discretization is shown in figure 1. Sensor displacements were considered to be in fixed and rotating coordinate systems with four sensors representing 2 planes. Auxiliary bearings are present in the model inside the active magnetic bearings and auxiliary bushes are present around the rotor in order to provide safety requirements (figure 1). Rotor control forces, **u**, are evaluated using a PID controller configured to provide rotor stability with minimum stiffness in order to minimize transmitted forces. The first four critical speeds of the rotor, configured with PID control, occur at 10Hz, 17Hz, 28Hz, and 67Hz. The first two are dominated by rigid body motion, while the two higher frequency modes involve significant flexure.

WAVELET ANALYSIS AND FILTER BANKS

Introduction to Wavelet Analysis

Wavelet analysis provides a multi-resolution time-frequency analysis of a signal through the evaluation of the signal with an appropriate mother wavelet, ψ, at different translations and dilations. This overcomes many of the problems associated with Fourier analysis such as fixed resolution and the evaluation of frequencies within a specific time window. This is achieved with a mother wavelet, $\psi(t)$, with zero mean:

$$\int_{-\infty}^{\infty} \psi(t)dt = 0 \tag{2}$$

The wavelet transform of a function $f(t)$ can now be written as:

$$c(a,b) = |a|^{-1/2} \int_{-\infty}^{\infty} f(t)\psi\left(\frac{t-b}{a}\right) dt \tag{3}$$

where a and b give the dilation and translation of the wavelet respectively. Since wavelets are localized in both time and frequency this relates to the time window and pseudo-frequency, which is dictated by the frequency content of the wavelet.

Discrete Time Wavelet Analysis

Through digital signal processing of a signal it is possible to obtain the wavelet transform coefficients, $c(a,b)$, on a discrete grid corresponding to the discrete time wavelet coefficients. This is achieved when a and b are assigned regularly spaced values: $a = ma_0$ and $b = nb_0$, where m and n are integer values. This is fully explained and developed in references [10, 11], however, an overview is given here for completeness. References [10, 11] show that a discrete time signal can be transformed into its discrete time wavelet series by being passed through high-pass and low-pass filters in parallel and downsampled by 2. The output signals are referred to as the approximate and detail coefficients respectively. It is the approximate coefficients that correspond to the discrete time wavelet coefficients. Successive wavelet decompositions can be obtained by repeating the filtering and downsampling (figure 2). Following the filter bank derivation in reference [11] it is possible to show that for a two channel orthogonal filter bank a single level wavelet decomposition takes the form of the convolutions:

$$h_0[n] * x[n]|_{n=2k} = X[2k] \tag{4}$$

$$h_1[n] * x[n]|_{n=2k} = X[2k+1] \tag{5}$$

where decomposition filters $h_0[n]$ and $h_1[n]$ represent the high and low pass filters respectively and have an impulse response specific to the choice of wavelet. Higher levels of coefficient are achieved from successive decompositions of the detail coefficient such that an output vector, $\mathbf{X}'$, of coefficients can be produced in the form:

$$\mathbf{X}' = \begin{pmatrix} X_1[2k] \\ X_2[4k] \\ \vdots \\ X_n[2^n k] \\ X_n[2^n k+1] \end{pmatrix} \tag{6}$$

where the subscript indicates the octave number. In contrast to Fourier analysis a wavelet approach is not restricted to a single basis set, but allows for the evaluation

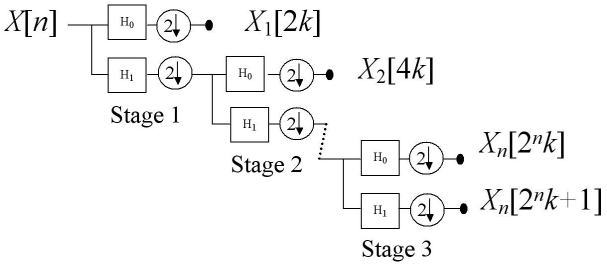

FIGURE 2: Wavelet decomposition filter bank.

of the wavelet transform coefficients with a variety of different wavelets. The different structures of the wavelets allow for a tailored approach to be taken when identifying different characteristics. A mother wavelet can be chosen to reflect the key artifacts associated with a specific fault disturbance.

The sample rate at any given sub-band, i, is given by 2^i since it is downsampled by 2 in each channel. This is called *Dyadic sampling*. Perfect signal reconstruction can be achieved through successive upsampling, filtering, with reconstruction filters, and summation of the coefficients with the detail signal.

The Haar Wavelet

There exist many different wavelets ranging in level of complexity. A choice must therefore be made as to which wavelet to use. Since this is focused on fault identification it makes sense to choose a wavelet to best reflect the fault conditions with the shortest duration, therefore maximizing detection speed. Consideration of sudden rotor unbalance and rotor/bearing contact faults are to be identified. The Haar wavelet is therefore a natural choice since it can be constructed from step changes resembling the sudden disturbances. The Haar basis, although simple, identifies key features such as periodic time variance and the relationship with filter bank analysis [11]. The Haar wavelet is also the simplest wavelet of the Daubechies family of wavelets [12], and can be expressed as:

$$\psi_{Haar}(t) = \begin{cases} 1 & 0 \le t < 1/2 \\ -1 & 1/2 \le t < 1 \\ 0 & \text{otherwise} \end{cases} \tag{7}$$

FAULT DISTURBANCE CLASSIFICATION

In order to maintain safe operation of a rotor/magnetic bearing system it is important to identify the onset time and disturbance type in order to evaluate the correct control forces. Correct identification of the disturbance from the response requires an understanding of both the system and the disturbance acting upon it.

Direct Synchronous Forcing

Direct synchronous forcing within the system arising from unbalance may be present at a residual level or it may occur suddenly. The most dramatic case is a step change. This can be represented in fixed or a synchronous rotating reference frames as:

$$f_x(t) + i f_y(t) = me\Omega^2 e^{i\Omega t} H(t-\tau) \tag{8}$$

$$f_u(t) + i f_v(t) = me\Omega^2 H(t-\tau) \tag{9}$$

where $H(t)$ is the Heaviside step function, m is the unbalance mass, e is the eccentricity and Ω is angular frequency of rotor rotation. f_x and f_y represent the forces in the directions of the x and y axes respectively. The forces f_u and f_v represent the components in the directions of the u and v axes, where the u and v are orthogonal in a rotational reference frame with a synchronous angular frequency. A rotating reference frame is a natural choice for the analysis of direct synchronous forcing since the force can be represented as a constant rather than an oscillation vector. The response of the rotor, $\mathbf{q}(t)$, can be described in both reference frames by:

$$\mathbf{q}(t) = \begin{cases} 0 & t < \tau \\ \mathbf{q}_{trans}(t) + \mathbf{q}_{ss}(t) & t \ge \tau \end{cases} \tag{10}$$

where $\mathbf{q}_{trans}(t)$ and $\mathbf{q}_{ss}(t)$ represent the transient and the steady state response respectively. In the case of a rotating reference frame the steady state response of the system is a constant. From equation (3) it is possible to take the continuous wavelet transform of rotor displacement, $\mathbf{q}(t)$, in the u and v directions at a specific element node. Defining some time T_{ss} to be the time at which the system reaches steady state and the transient response becomes negligible, then for a single degree of freedom:

$$c(a,b) = \begin{cases} 0 & b < \tau - a \\ \int_{-\infty}^{\infty} q_{trans}\psi(\frac{t-b}{a})dt & \tau - a \le b < T_{ss} + \tau \\ 0 & T_{ss} + \tau < b \end{cases} \tag{11}$$

Therefore in a rotating reference frame, since a wavelet has zero mean, the wavelet coefficients only have non-zero values in the region of transient response.

Auxiliary Bearing Contact

Auxiliary bearing contact with the rotor may occur from a wide variety of fault conditions. In order to identify contact from a sensor signal it is important to understand the system dynamics. The force exerted by the auxiliary bearing on the rotor, during a short duration contact, normal and tangential to contact may be written as:

$$f_x(t) + i f_y(t) = [-f_c - i\mu f_c] P(t) e^{i\theta} \tag{12}$$

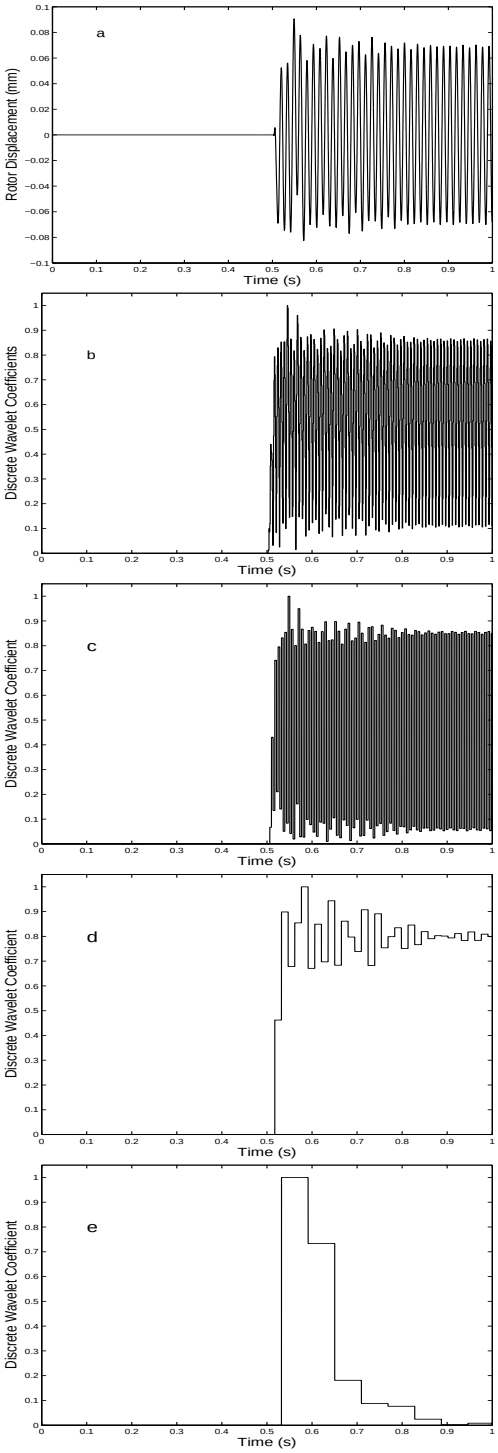

FIGURE 3: Rotor displacement in the x direction at sensor 1 due to sudden unbalance, (a). Absolute normalized discrete time wavelet series of rotor displacement during direct synchronous forcing in a fixed reference frame at the second flexural mode at the 1^{st} (b), 3^{rd} (c), 5^{th} (d), and 7^{th} (e), octaves.

where μ is the friction coefficient of contact, θ is a phase angle and f_c is the radial force acting on the rotor from

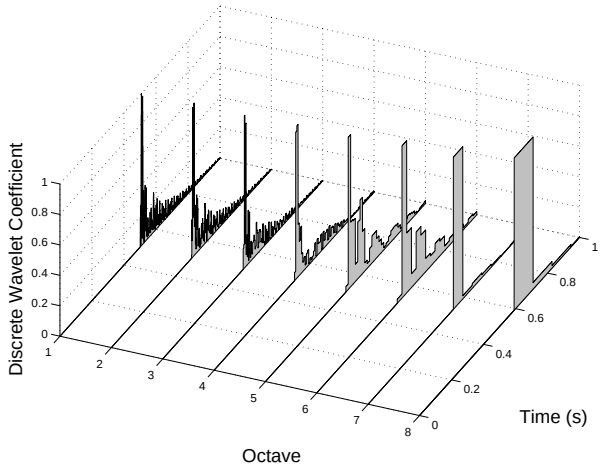

FIGURE 4: Absolute normalized discrete time wavelet series of rotor displacement during a sudden change in direct synchronous forcing in a rotating reference frame at the second flexural mode.

the auxiliary bearing. $P(t)$ is a parameter representing the contact period and is zero when contact no occurs. This was based on Hertzian stresses.

The rotor response to the short duration contact in both the fixed and rotating reference frames will take the form of equation (10). Therefore, a wavelet analysis of the rotor displacement will contain non-zero wavelet coefficients during the transient response only, shown in equation (11). However, unlike sudden unbalance the wavelet coefficients will be localized in the rotating reference frame.

SIMULATION

Simulation of the rotor response to the different fault conditions was undertaken over a range of running speeds up to and including the natural frequency of the second bending mode (67Hz). The wavelet decomposition filter banks were configured with a wavelet sampling frequency of 0.46ms, matching the synchronous frequency at the 5^{th} octave. The filter banks were configured with a frequency range of eight octaves. This provides information of frequencies both higher and lower than the running speed of the rotor. A rotor unbalance response was obtained by applying a synchronous disturbance force to the right hand end of the rotor equivalent to 300N amplitude (figure 1). Wavelet analysis was undertaken on the rotor displacement at sensor 1, in order to demonstrate non-local fault detection. The octaves have been numbered such that highest frequency is number one.

The rotor response at a frequency of 67Hz, corresponding to the natural frequency of the second bending mode, is presented in figure 3. Figure 3a shows the rotor undergoing a transient period before settling into a steady state vibration. This is further seen in figure 3d at the 5^{th}

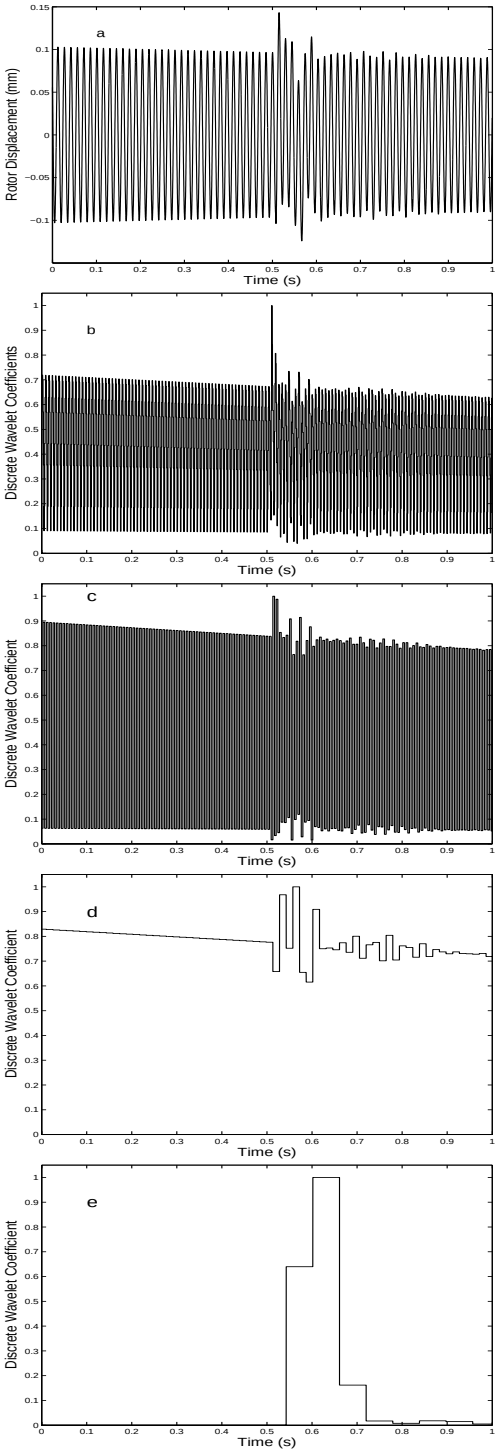

FIGURE 5: Rotor displacement in the x direction at sensor 1 due to sudden unbalance, (a). Absolute normalized discrete time wavelet series of rotor displacement during rotor/bearing contact in a fixed reference frame at the second flexural mode at the 1^{st} (b), 3^{rd} (c), 5^{th} (d), and 7^{th} (e), octaves.

octave, matching the synchronous frequency. In a rotating reference frame the wavelet coefficients only have non-zero values in the region of the transient response.

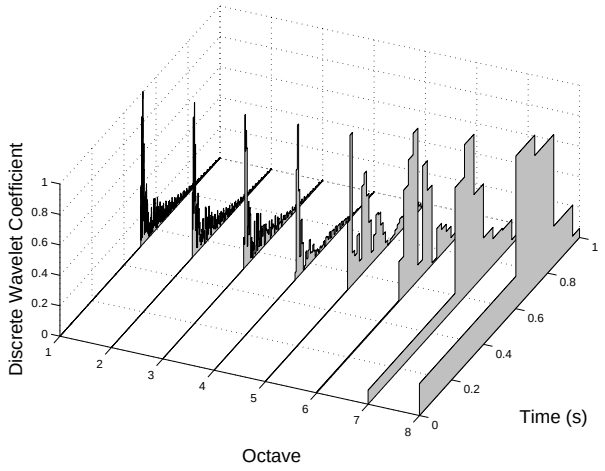

FIGURE 6: Absolute normalized discrete time wavelet series of rotor displacement during rotor/auxillary bearing contact in a rotating reference frame at the second flexural mode.

This is seen in figure 4 showing peaks in the coefficients immediately after the onset of direct synchronous forcing. It is clear from figures 3 and 4 that high and low frequencies are excited by the sudden change in forcing condition on the rotor. In a rotating reference frame the wavelet coefficients are present immediately after the disturbance before decaying. In the fixed reference frame the low frequencies are seen to decay while frequencies higher than and including the synchronous frequency remain. The response time of the different octaves to the fault is dependent on the sampling frequency such that the higher octaves, lower frequencies, take longer to resolve.

In order to identify artifacts due to rotor/auxiliary bearing contact the rotor needs to be in steady state so that any artifact associated with changes in the forcing will have decayed. Auxiliary bearing contact was made with a steadily orbiting rotor, undergoing direct synchronous forcing slowly reducing with time, in order to demonstrate the ability of wavelet analysis to detect the sudden contact and the general behavior of the rotor. Contact was achieved through progressive misalignment of the right hand bearing (figure 1) until contact occurred. Immediately after contact the bearing was returned to its original location in order to prevent further contacts. Direct synchronous forcing was used to excite the rotor into a steady state orbit so that a comparison can be made between the wavelet coefficients of both faults allowing for them to be distinguished. Simulation of the rotor/bearing contact shows the short duration contact assumption to be reasonable with simulation contact time lasting $\sim 1/20^{th}$ of a rotor period.

Figure 5 shows the wavelet coefficients evaluated in a fixed reference frame at the 1^{st}, 3^{rd}, 5^{th} and 7^{th} octaves. Localized excitation of the wavelet coefficients due to the contact is clearly visible. This is further

seen in figure 6 showing localized excitation of high and low frequency wavelets coefficients immediately after rotor/bearing contact. However, in a fixed reference frame residual wavelet coefficients associated with the steady state rotor orbit are also present in the wavelet coefficients corresponding to frequencies higher than and including the rotor speed (figure 5).

Figures 3, 4, 5 and 6 show that the onset time of both sudden unbalance or rotor/bearing contact can be identified. Furthermore, the induced wavelet coefficients due to a rotor/bearing fault condition are only present for a short period in both reference frames. However, sudden rotor unbalance leads to short duration coefficients in the rotating reference frame only and a steady vibration in the fixed reference frame. Therefore it is also possible to differentiate between fault conditions as well as identify the onset time.

CONCLUSIONS

A digital signal processing approach was undertaken to identify the discrete time wavelet coefficients of rotor displacement through filter bank analysis in order to ascertain fault onset and type. From an understanding of the fault condition specific artifacts associated with it can be identified within the wavelet coefficients. The Haar wavelet was chosen as the mother wavelet since its shape is suited for step changes in unbalance and short duration contacts.

Consideration of sudden rotor unbalance indicates that in a synchronous rotating reference frame wavelet coefficients will only be non-zero during the transient response of that frequency. In the case of rotor/bearing contact it has been argued that non-zero coefficients will also only be present during the transient response. However, in the contact case this is argued to be independent of the reference frame, therefore the fault types can be distinguished.

Simulations of a flexible rotor/magnetic bearing system were undertaken at running speeds up to and including the natural frequency of the second flexural mode of vibration occurring at 67Hz. Rotor displacement resulting from direct synchronous forcing due to a sudden unbalance was shown to contain localized high and low frequency wavelet coefficients in a rotating reference frame. It was also possible to detect the rotor orbit at a wavelet coefficient comparable to the synchronous frequency. Rotor/bearing contact was achieved through bearing misalignment until contact with a steady state rotor orbit. High and low frequency vibrations were detected in both the fixed and rotating reference frames along with the synchronous vibrations due to synchronous forcing. The onset time of both fault conditions was easily detected. Identification of the fault condition can be made from a comparison between the reference frames of the faults.

ACKNOWLEDGMENTS

The authors gratefully acknowledge the funding support of the Engineering and Physical Sciences Research Council through grant GR/R45277/01.

REFERENCES

[1] **M.O.T. Cole, P.S. Keogh and C.R. Burrows.** Fault-Tolerant Control of Rotor/Magnetic Bearing Systems Using Reconfigurable Control with Built in Fault Detection, *Proc. I. Mech. E., Part C, Journal Mechanical Engineering Science*, 2000, **214**, 1445-1465.

[2] **C. Seo and B.K. Kim.** Robust and Reliable H_∞ Control for Linear Systems with Parameter Uncertainity and Acuator Failure. *Automatica*, 1996, **32**(3), 465-467.

[3] **A.N. Gündes** Stabilizing Controller Design for Linear Systems with Sensor or Actuator Failures. *IEEE Transactions on Automatic Control*, 1994, **39**(6), 1224-1230.

[4] **D. Sauter and F. Hamelin** Frequency-Domain Optimization for Robust Fault Defection and Isolation in Dynamic Systems. *IEEE Transactions on Automatic Control*, 1999, **44**(4), 878-882.

[5] **Y. Maki and K.A. Loparo.** A Neural-Network Approach to Fault Detection and Diagnosis in Industrial Processes. *IEEE Trans. Control Sys Technol.*, 1997, **5**(6), 529-541.

[6] **N. Bachschmid, P. Pennacchi and A. Vania.** Identification of Multiple Faults in Rotor Systems. *Journal of Sound and Vibration*, 2002, **254**(2), 327-366.

[7] **Z. Peng, Y. He, Q. Lu and F. Chu.** Feature Extraction of the Rub-Impact Rotor Systems by Means of Wavelet Analysis. *Journal of Sound and Vibration*, 2003, **259**(4),1000-1010.

[8] **J. Lin and L. Qu,** Feacture Extraction Based on Morlet Wavelet and its Application for Mechanical Fault Diagnosis. *Journal of Sound and Vibration*, 2000, **234**(1),135-147.

[9] **D.E. Newland** Wavelet Analysis of Vibration, Part 2: Wavelet Maps. *ASME Journal of Vibration and Acoustics*, 1994, **116**, 417-425.

[10] **G. Strang and T. Nguyen,** 1996, *Wavelets and Filter Banks*. Wellesley-Cambridge Press, Cambridge, MA.

[11] **M. Vetterli and J. Kovacevic,** 1995, *Wavelets and Subband Coding*. Prentice Hall, Inc. New Jersey.

[12] **I. Daubechies,** 1992, *Ten Lectures on Wavelets*. Society for Industrial and Applied Mathematics (SIAM), Pennsylvania.